crystals

MDPI

Article

Rapid Growth of KDP Crystals in the [101] Direction

Mengfei Qin [1,2], Xinguang Xu [1,2,*], Guangwei Yu [1], Bo Wang [1,2] and Wenyong Cheng [1]

1 State Key Laboratory of Crystal Materials, Shandong University, Jinan 250100, China; 201411953@mail.sdu.edu.cn (M.Q.); gwyu@sdu.edu.cn (G.Y.); wangbo1010@sdu.edu.cn (B.W.); cwy@sdu.edu.cn (W.C.)

2 Key Laboratory of Functional Crystal Materials and Device, Ministry of Education, Shandong University, Jinan 250100, China

* Correspondence: xgxu@sdu.edu.cn

Received: 18 January 2020; Accepted: 10 February 2020; Published: 12 February 2020

check for updates

Abstract: KDP crystals have important applications in inertial confinement fusion. However, during the rapid growth of large-sized KDP crystals, inclusion is prone to occur. The existence of inclusion will lead to the reduction of crystal quality and utilization and even the end of the growth process. The generation of inclusion is related to the interaction between the crystal and the liquid flow. In this paper, we changed the hydrodynamic condition around the crystal by changing the crystal growth direction and achieve the rapid growth of [101] direction KDP crystals without inclusion at a low rotation rate. The utilization of the crystal was improved and the crystal has good optical transmittance, crystalline perfection and laser damage threshold. Meanwhile, atomic force microscopy was used to study the characteristics and changes of the micromorphology on (100) and (101) faces under different levels of supersaturation. The analysis results show that under high supersaturation, the uneven distribution of solutes and insufficient flow rate cause local macrosteps, two-dimensional step platforms and two-dimensional cores to form irregular structures with large slopes, thereby reducing the stability of the interface. This study will help to better understand the effect of the interaction between liquid flow and crystals on the formation of inclusion and guide the growth of KDP crystals.

Keywords: KDP crystals; rapid growth; AFM; growth mechanism; inclusion; optical performance

1. Introduction

Potassium dihydrogen phosphate (KH_2PO_4, KDP) crystal is a representative electro-optical conversion and nonlinear optical material which could be grown into large size in aqueous solution. With the development of laser fusion, KDP crystal is used in the inner confinement fusion (ICF) project for pockels cell and frequency conversion. As the laser energy increases, more and more KDP optical elements are needed. To meet the quantity demanded, a lot of work had been done to shorten the growth period of traditional techniques [1]. A.A. Chernov, N.P. Zaitseva and L.N. Rashkovich achieved rapid growth of a point seed KDP crystal by using a standard Holden-type crystallizer with reversible rotation, the highest growth speed could reach 70 mm/day [2]. N.P. Zaitseva developed the point seed rapid growth method and achieved the growth of large-type (400–550 mm) KDP crystals [3]. As the crystal size increases, solution inclusion frequently occurs inside, which limit the optical performance and yield. Many researchers have shown that the formation of solution inclusion is connected with supersaturation inhomogeneity and morphological instability [4–8], A.A. Chernov investigated the process of steps movement and bunching, solution disturbance could influence the move speed and density of elementary steps and results in the formation of macrosteps, distribution difference of supersaturation in steps region accelerate the formation of macrosteps. The development of macrosteps may cause the instability of surface morphology and result in the solution inclusion [9]. Serge Yu.

Potapenko analysed the interaction of solution flow and step associated with lateral perturbations and the formation of solution inclusion, it was found that the steps bunching and lateral instabilities result in the structure of solution inclusion [10,11]. Harry F. Robey observed the structure of macrosteps and lateral instability [12] by optical and interferometric microscope, the measurement of surface slopes distribution showed the morphological instability was connected with the vicinal slope which caused by "step-bending" [13]. He simulated the hydrodynamics and mass transfer of large type rapid grown KDP crystals, the distribution of surface shear stress and supersaturation was performed to better understand the inclusion formation and morphological instability process associated with growth parameter [14]. Peter F. Bordui and Shahryar Motakef confirmed the instability of KTiOPO4 (KTP) crystal interface by experiments of visible liquid flow and growth of crystals in different directions. They pointed out that the inclusion formation is related to the non-uniformity of the crystal surface supersaturation, the effect of uneven concentration of the solution near the crystal is governed by the morphology of the crystal face [15]. Bhushan Vartak used finite element numerical simulation to calculate the three-dimensional solution flow, material transport and continuous growth kinetics during KTP crystal growth. The flow field and crystal surface solution concentration distribution were analyzed by changing the crystal orientation, and 90 degree placement was found to facilitate the mixing of the solution and the uniform distribution of supersaturation, which is more conducive to the growth of the crystal [16]. At the same time, a lot work have been done to improve the yield and quality of KDP crystals by changing the growth method or seed orientation [17–20], He Youping and V.I. Salo have grown high quality and availability KDP crystals by using (101) plane seeds, the regeneration process can be avoided and the utilization can be increased up to 40%~70% for KDP and DKDP [21,22].

To investigate the causes of inclusion formation and avoid it effectively, a series of [101] orientation KDP crystals were grown by point seed rapid growth method, the surface microtopography of (100) and (101) faces under different supersaturation were measured by atomic force microscope (AFM), the growth habit, optical transmittance, crystalline perfection and laser damage threshold of grown crystals have also been characterized.

2. Materials and Methods

All the growth of KDP crystals was performed in a 5000 mL standard growth device, the temperature of the waterbath is well controlled by Shimaden Fp23 temperature controller with an accuracy of ±0.01 °C. The periodically reversible rotation speed of crystal platform was set as 30 rpm (Revolutions Per Minute), the growth aqueous solution was prepared by high purity KDP raw materials and deionized water, then purified through two layers of filter membrane with pore diameters of 0.1 and 0.05 μm, then overheated at 15 °C above the saturation temperature over 12 h. The [101] direction point seed was fixed on the growth platform, when the temperature of solution was reduced to 2 °C above the saturated point, the growth platform was introduced into the growth solution, then the temperature was kept 0.5 °C below the saturation point for the seed to regeneration. After the regeneration, the temperature was cooled to different values, the crystal was kept at that supersaturation to grow for about 1 day, then the crystal was disposed by mixed solution of water and alcohol to remove the residual solution and the surface was dried by strong absorbent paper, the mass ratio of water to alcohol is 9:1, the whole process takes less than 5 s and send it right away for testing. The saturation point of the solution was measured before and after the growth and the difference was very small, so the bulk supersaturation of the solution was considered constant. The value of supersaturation is calculated according to Equation (1),

$$\sigma = \frac{c - c_e}{c_e} \times 100\% \quad (1)$$

where c is the real concentration of solution, c_e is the concentration of solution under equilibrium temperature. The pH value of solution at 55 °C is 3.8.

In this work, a series of [101] direction KDP crystals were grown for surface microtopography detection, the growth supersaturation range were from 0.37% to 8.09%. The AFM was manufactured by Veeco Instruments Company and the model is Dimension Icon. The imaging range is 70 μm × 70 μm × 5 μm, the lateral resolution is 0.1 nm, the longitudinal resolution is 0.01 nm, and the images were obtained in tapping mode. Large size [101] direction KDP crystals were grown by point seed rapid growth method and the performance has also been investigated. The 200–1800 nm wavelength spectrum transmittance was measured by UH4150 spectrophotometer at room temperature, and the rocking curve of (001) face was measured by D5005HR type single crystal high resolution X-ray diffractometer made by Bruker-axe company, the monochromator consists of four highly complete U-type Ge (220) single crystals. The X-ray tube is a Cu target, and CuKα1 (λ = 0.15485 nm) beam was obtained to use as X-ray beam, the test accuracy is 0.0001°. The laser damage threshold of Z-cut plate was also tested by 1064 nm Nd: YAG laser, the repetition frequency is 1 Hz, the pulse width is 8.4ns and target surface area is 0.2 mm^2, the test mode is 1-on-1.

3. Results and Discussion

3.1. (100) Surface Microtopography under Different Supersaturation

To determine the comprehensive microtopography information about (100) faces, many KDP crystals were grown and a lot of position on the two sides were measured, the representative images are shown in Figure 1, the corresponding steps height and width are shown in Figure 2.

Figure 1a shows the image of steps under 0.38% supersaturation, most elementary steps were uniform distributed in this region (Figure 2a), the height of elementary steps is between 0.512 nm and 0.588 nm, the width is about 150 nm, only a few steps have large widths over 500 nm. According to the AFM measurement of T.N. Thomas [23], the height of elementary steps on the (100) is 0.37 nm, which corresponds to half of the unit cell height, so we measured many locations in the picture. The height of elementary steps on the (100) face is between 0.371 nm and 0.588 nm, most are about 0.4 nm, this may be caused by differences in growth conditions and deviations in measurements. Figure 1b is the picture of macrosteps train on the (100) surface when the supersaturation is 0.74%, the contour of steps is not regular and the edge is jagged. The height of macrosteps is between 25.6 nm and 36.3 nm (Figure 2b), steps are evenly distributed. It seems some elementary steps are stacking on the surface of macrosteps, but the clear structure cannot be seen when magnify this region. The same microtopography was also observed when crystal grew under 3.94% supersaturation, as shown in Figure 1c, macrosteps become larger and wider, the step height is between 97.1 nm and 133 nm (Figure 2c). The surface structure of macrostep can be seen clearly, as shown in Figure 1d, the elementary steps are stacking on the surface and the step edge is round.

When the growth supersaturation increased to 5.99%, regular macrosteps made up of elementary steps were observed; nevertheless, some irregular structures were observed. As shown in Figures 1e and 2d, the microtopography is disorder, compared to the previous step distribution, macrosteps have large differences in height and width, the height of these structures is between 61.6 nm and 128 nm. Some structures are confirmed to be made up of elementary steps, other special structures on the surface of macrosteps are shown in Figure 1f, a convex and circular platform stacked by elementary steps on the top of macrosteps, a few step surfaces with different heights are on the top of it. When the growth supersaturation increased to 8.09%, big macrosteps were observed and difference of height and width is more obvious (Figure 2e), from 56.2 nm to 167 nm, the width can reach to 28.63 μm. Surfaces of some macrosteps become rough, irregular island patterns appear on it, as shown in Figure 1g. A dendritic pattern was magnified as Figure 1h shows, it can be seen this structure was formed by many stacked elementary steps, their heights are higher than the surface. These steps were not homogeneous distribution and porous structures were among them.

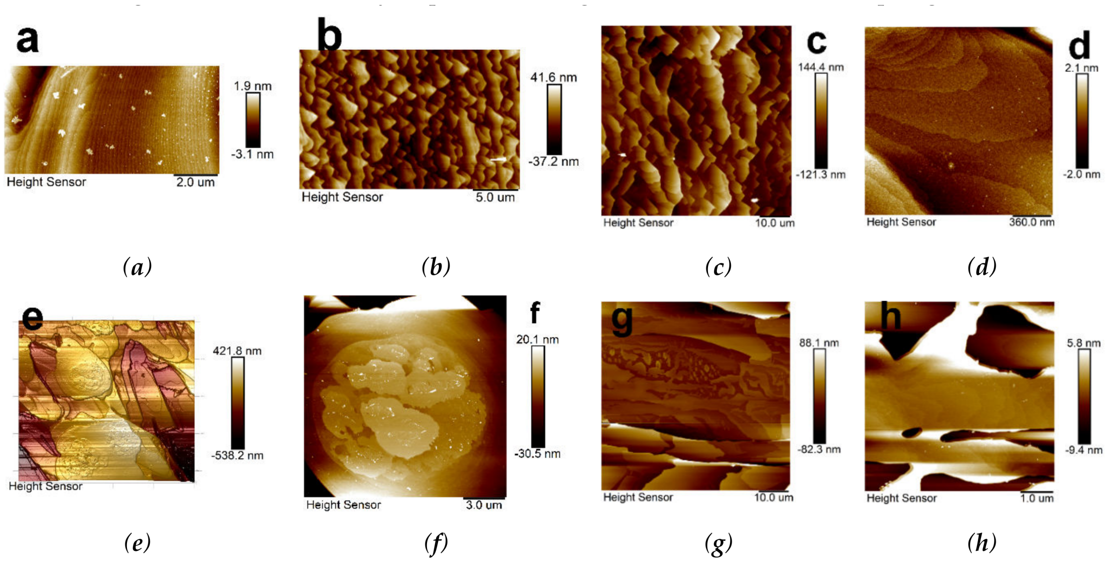

Figure 1. Microtopography of (100) faces of KDP crystals grown in [101] direction under different supersaturation: (**a**) σ = 0.38%; (**b**) σ = 0.74%; (**c**), (**d**) σ = 3.94%; (**e**), (**f**) σ = 5.99%; (**g**), (**h**) σ = 8.09%.

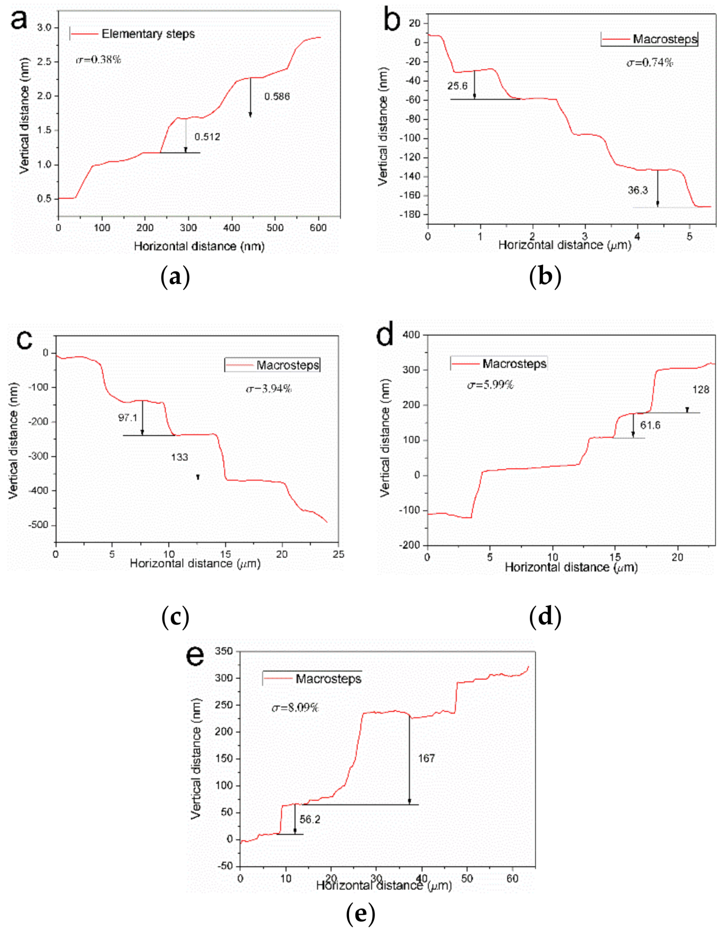

Figure 2. Steps profile images measured by AFM under different supersaturation: (**a**) σ = 0.38%; (**b**) σ = 0.74%; (**c**) σ = 3.94%; (**d**), σ = 5.99%; (**e**), σ = 8.09%.

Many studies have shown that supersaturation, impurity and PH are the main parameters affecting the growth rate of the (100) face of KDP crystals [24–26], since the same batch of KDP raw materials were used in the experiment, the types and contents of impurities and PH were at the same level, so the supersaturation became the only factor affecting growth rate. The step growth rate experiences a dead zone, a nonlinear increase and a linear increase phase as the supersaturation increases, elementary steps and macrosteps motion is involved in this process. During the (100) face microtopography study of rapid growth [101] direction KDP crystals, morphology of elementary steps and macrosteps were observed from low supersaturation to high supersaturation, the elementary steps were regular and parallel distribution when supersaturation was low, the shape of the macrostep is jagged and height and width increase as supersaturation increases.

When the supersaturation was high enough, irregular distribution of macrosteps with different height and width appeared on the (100) face of the crystal, the surface slope increased, and resulting in the increase of morphological instability. The morphological stability of a face is determined by the supersaturation distribution over the surface [12] and the supersaturation gradient normally to it [27]. During the rapid growth process, supersaturation distribution of (100) face is inhomogeneous due to the varying boundary layer thickness on surface. Uneven distribution of supersaturation on the surface would cause different growth rate of the local step, stagnation of elementary steps propagation, formation of macrosteps and steps "bending" [28]. During the growth of KDP crystals, the rotation rate was fixed, so the flow rate and the thickness of the diffusion layer was constant, as the increase of supersaturation, the supersaturation gradient increased and the flow rate was insufficient to support the movement of step train, then the longitudinal instability and lateral instability developed, the surface became unstable [29]. As Figure 2d,e show, which may cause the instability of surface and develop into defects such as holes or inclusion as this situation continues. Therefore, it is necessary to maintain proper supersaturation when growing KDP crystals at low rotational speeds.

3.2. (101) Surface Microtopography under Different Supersaturation

Due to the [101] direction growth of KDP crystal, the top (101) face can be measured directly by AFM without any other adjustment. A series of crystals were grown under different supersaturation for AFM measurement, the microtopography of (101) face was measured from low to high supersaturation and special structures have also been investigated.

3.2.1. Microtopography under Low Supersaturation

Figure 3 is the microtopography of (101) faces under 0.37%–1.87% supersaturation, and the corresponding step information is shown in Figure 4. It can be seen from Figure 3a that tiny steps were densely distributed in all the region when supersaturation is 0.37%, Figure 3b is the magnified area, the height of elementary step is between 0.383 nm and 0.515 nm, the width is 30 nm (Figure 4a), no step bunching was found. According to the measurement of J.J. De Yoreo [30], the height of elementary steps on the (101) face is 0.5086 nm, which is in a good agreement with the interplane distance d = 0.507 nm. The same steps distribution was also observed when crystal grew under 0.74% supersaturation, Figure 3c shows a neat arrangement of steps, the height of step is about 0.547 nm and the width is between 60 nm and 150 nm, meanwhile a special triangular pit pattern was observed, as shown in Figure 3d. This structure was formed by three macrosteps in three directions, as shown in Figure 4b, the height of them is between 19.763 nm and 67.687 nm, the right side is taller than the other two sides. A growth hillock was found in the middle of the pit, the hillock is formed by bunches of steps and two-dimensional nucleuses appear on the top of it, as shown in Figure 3e. When the growth supersaturation increased to 1.87%, neat arrays of elementary steps was observed on the surface as shown in Figure 3f, the average value of height and width is about 0.43 nm and 70 nm, no step bunches was found. A special triangular pattern was found, Figure 3g shows the detail of the structure, it was formed by three faces at angles to each other macroscopically. Figure 3h shows the structure of one face, it was a bluff macrosteps made up of a lot of stacked steps, Figure 4c shows the profile of the steps, the height of the left and right macrosteps is 30.076 nm and 31.072 nm respectively. Elementary steps were observed on the bottom of that pit and their orientation is different from the two macrosteps, elementary step bending was found at the juncture of each other.

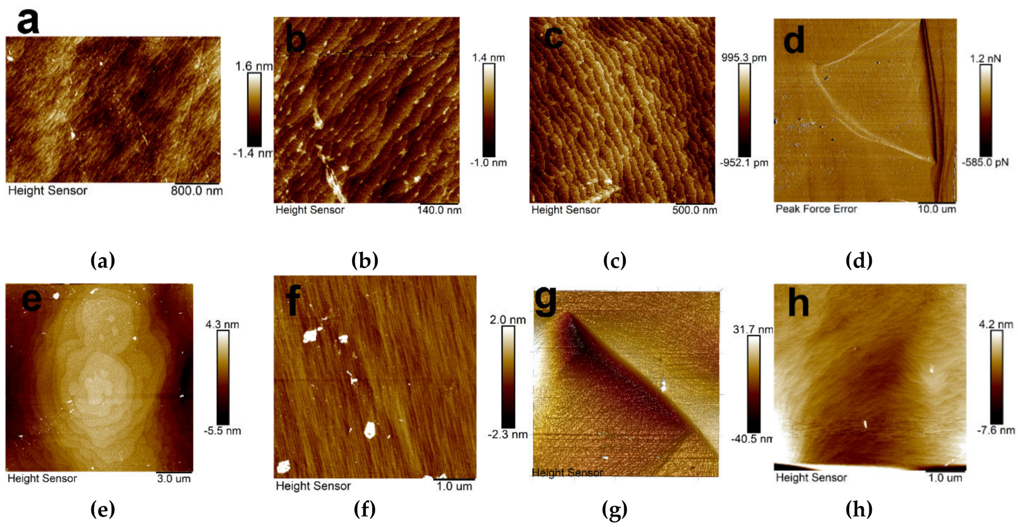

Figure 3. Microtopography of (101) faces of KDP crystals grown in [101] direction under low supersaturation: (**a**), (**b**) σ = 0.37%; (**c**), (**d**), (**e**) σ = 0.74%; (**f**), (**g**), (**h**) σ = 1.87%.

Compared with the (100) face of KDP crystal, the elementary step of the (101) face does not show a tendency to aggregate under low supersaturation; this may be related to structural differences between the prismatic and the pyramidal faces [31], the termination of K+ on the (101) face make the metal impurities harder to adsorb and block the growth of steps. The only step bunching was observed in the triangular pit, elementary steps were bended and bunched into macrosteps on the edge of the pit, two-dimensional growth hillock platform was founded in the middle of the pit and two-dimensional nucleation was founded on the top of it, which means that the supersaturation around was high enough to support the nucleation growth.

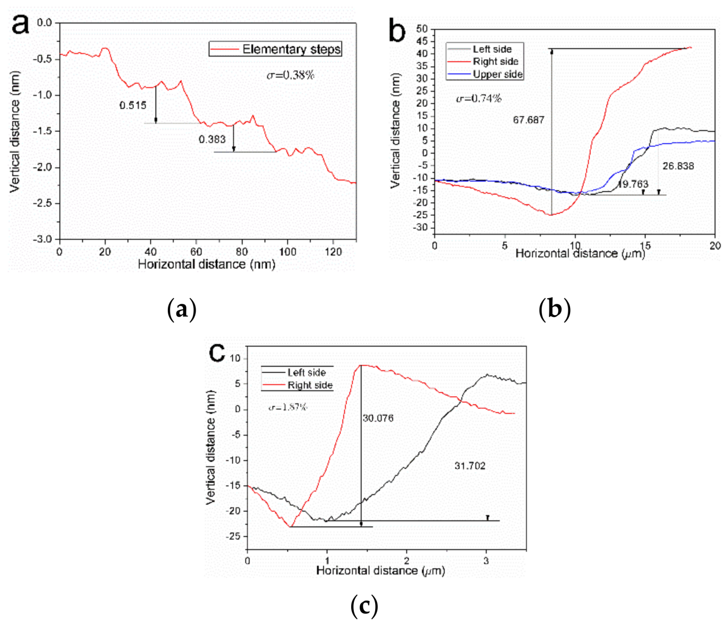

Figure 4. Steps profile images measured by AFM under different supersaturation: (**a**) σ = 0.38%; (**b**) σ = 0.74%; (**c**) σ = 1.87%.

3.2.2. Microtopography under High Supersaturation

Figure 5 is the surface microtopography of (101) faces when growth supersaturation was 3.94%–8.09%, the image is a little different from the Figure 3, more macrosteps were observed on the surface. Figure 5a is a 58.7 × 58.7µm microtopography image under 3.94% supersaturation, marosteps were not parallel distributed, significant differences in height and width were found according to the step profile measurement, the result is shown in Figure 6a. There are round and straight two types macrosteps patterns, Figure 5b is the structure of magnified round macrostep, it was formed by round and stacked elementary steps, two-dimensional cores were distributed on the top of wide steps, they grew and gathered into steps. Figure 5c shows the microtopography of two straight macrosteps, the left one was formed by many parallel elementary steps, two-dimensional cores were distributed on the top of the right macrosteps. More unstable surface morphology were observed when crystal grew under 5.99% supersaturation, Figure 5d shows a kind of wrinkle structure on the surface, the height and width of it are shown in Figure 6b, a cliffy hillock with height of 62.169 nm appeared on the surface, Figure 5e is a magnified image of one unstable region, a round platform formed by step bunches was on the top, two-dimensional cores were observed on the surface of top step and other wide steps.

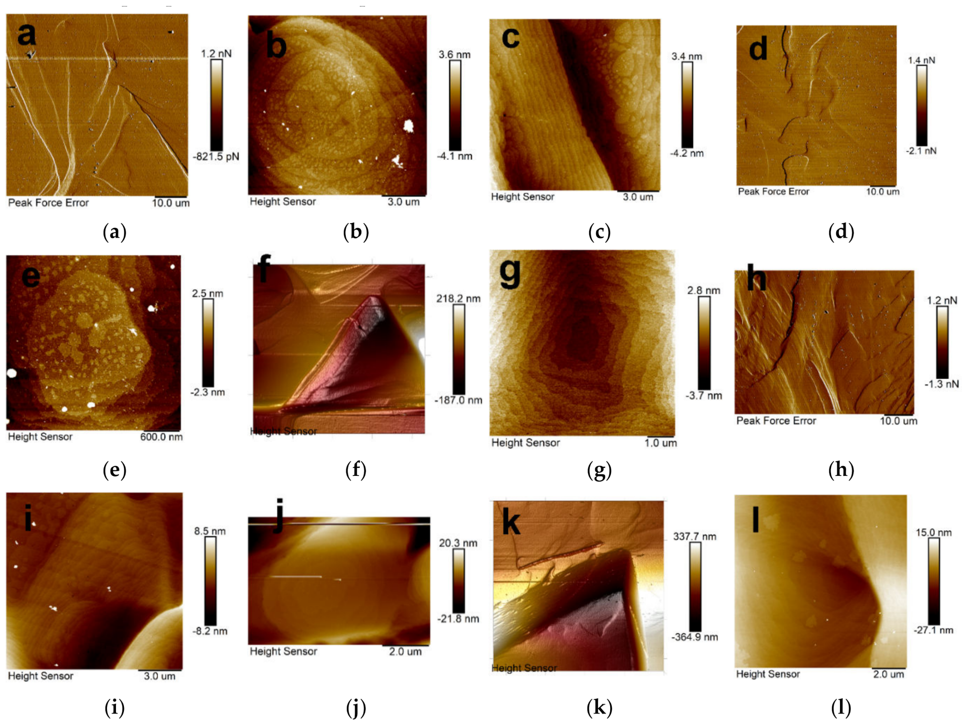

Figure 5. Microtopography of (101) faces of KDP crystals grown in [101] direction under high supersaturation: (**a**), (**b**), (**c**) σ = 3.94%; (**d**), (**e**), (**f**), (**g**) σ = 5.99%; (**h**), (**i**), (**j**), (**k**), (**l**) σ = 8.09%.

A triangular pit was also founded on the surface, Figure 5f is the three-dimensional diagram of the triangular pit, it was surrounded by three macrosteps in different directions, the height of macrosteps is about 130 nm, elementary steps finally converged at one point on the bottom of pit. Figure 5g is the intersection image of elementary steps, elementary steps of differernt directions were combined with each other by bending from the bottom to the top. The surface microtopography got more complicated when crystal grew under 8.09% supersaturation, as shown in Figure 5h, microstructures haphazardly distributed and surface is uneven, detail step profile is shown in Figure 6c, this region has large fluctuations, the height difference is between 43.476 nm and 91.884 nm. Figure 5i,j were the magnified microstructure, Figure 5i shows the elementary steps distribution, the bottom part is flat and the higher part is steep, the height different can reach to 9.842 nm and two-dimensional nucleuses distributed on some steps. Figure 5j shows a round platform formed by steps bunches, small island nucleuses spread evenly on the top. The triangular pit was also observed under this supersaturation, Figure 5k shows the 3D structure of it. Two macrosteps and the bottom face were founded converged at one point, Figure 6d shows that the macrosteps have different height and slope, the right one is taller and steeper than the left one. A pit was observed on the bottom face, the magnified detail image is shown in Figure 5l; it is a circle structure formed by bended elementary steps from macrosteps in three different direction.

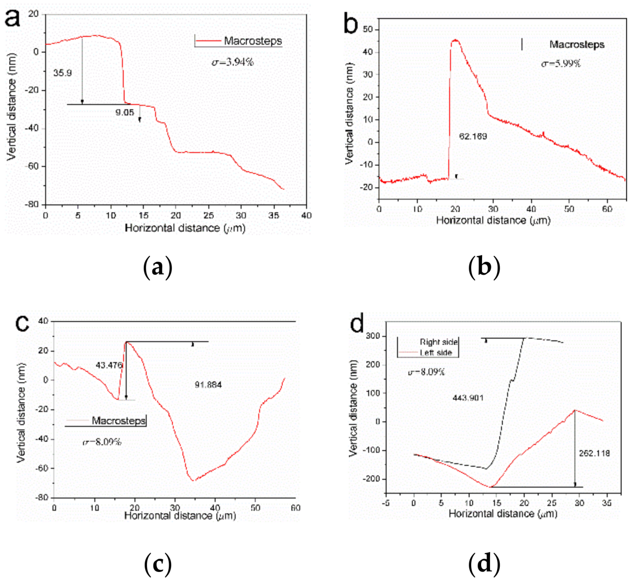

Figure 6. Steps profile images measured by AFM under different supersaturation: (**a**) σ = 3.94%; (**b**) σ = 5.99%; (**c**) (**d**) σ = 8.09%.

During the growth of [101] direction KDP crystals, some irregular microstructures appeared on the (101) face when the supersaturation was high, relative to other areas, they have a higher height and a larger slope and mainly composed of elementary steps and two-dimensional step bunching platforms, two-dimensional cores were selectively distributed on the top of them, which indicates the supersaturation was higher in this region. The (101) faces are perpendicular to the axis of rotation, so the flow pattern is similar to the von Kármán driven by a rotating disk [16]. The flow above the (101) face is weak in mixing; under these circumstances, the thickness of the diffusion layer is constant over the entire surface. Therefore, the hydrodynamics play a decisive role on the surface morphology. According to the analysis of the effect of a parallel shear flow and anisotropic interface kinetics [32], the direction of shear flow relative to the step motion affects the surface stability. During the growth KDP crystals at low supersaturations, the reversed periodically rotation and sufficient flowrates make the interface stable. As the increase of supersaturation, the flowrates become insufficient to support the step motion, then the longitudinal instability and lateral instability appeared and resulted in step bunching and modulations. Meanwhile, high bulk supersaturation made the supersaturation gradient greater, the stability of surface morphology decreased. The propagation of macrosteps and the amplification of instabilities contribute to the formation of inclusion [12,29]. To avoid the growth of instabilities and increase the stability of surface, the crystal should grow under proper supersaturation range when the rotation rate is low.

3.3. Triangular Pit Microtopography Revealed on the (101) Surface

During the process of KDP sample treatment, the crystal surface is so sensitive to the treating fluid that the microtopography could be destroyed and etch pits will appear on the surface, as shown in Figure 7a, the shape of etch pits looks like triangle, Figure 7b shows the 3D topography image measured by AFM, three faces in different directions converge at one point, the detail of microtopography have been wiped and the only thing can be distinguished is the macrostructures arranged in different orientation on the three surface. Figure 8a shows the height profile of the three faces, three faces have different slopes and their height gradually increases from the bottom.

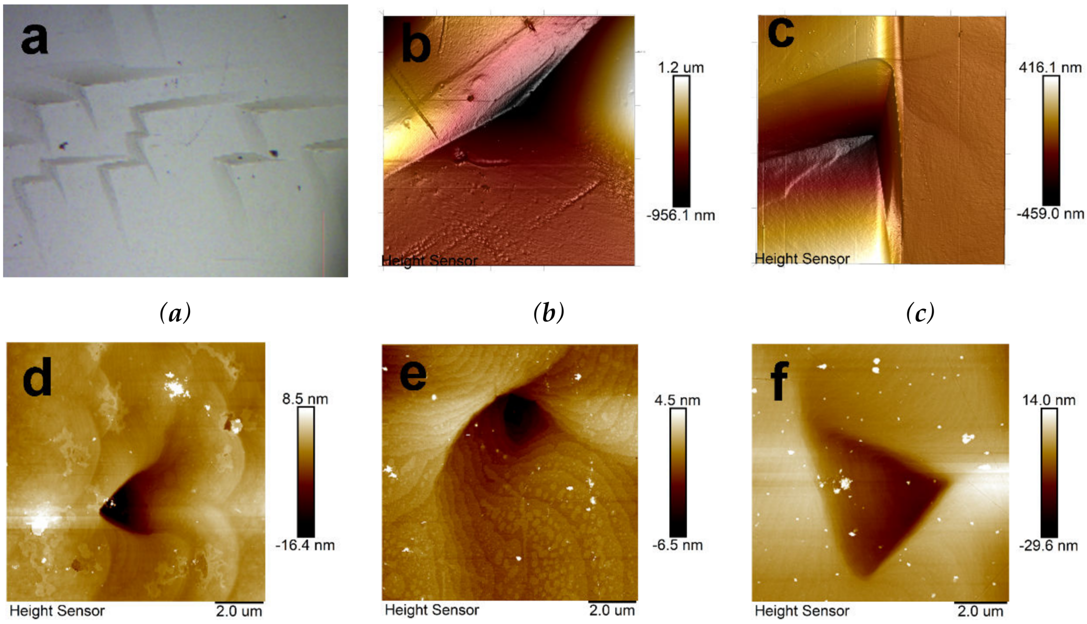

(a) *(b)* *(c)*

(d) *(e)* *(f)*

Figure 7. Microtopography of (101) faces of KDP crystals grown in [101] direction under different supersaturation: (**a**) photo of etch pit; (**b**) 3D image of etch pit; (**c**) 3D image of triangular pit; (**d**), (**e**), (**f**) morphology of triangular pit under different supersaturation.

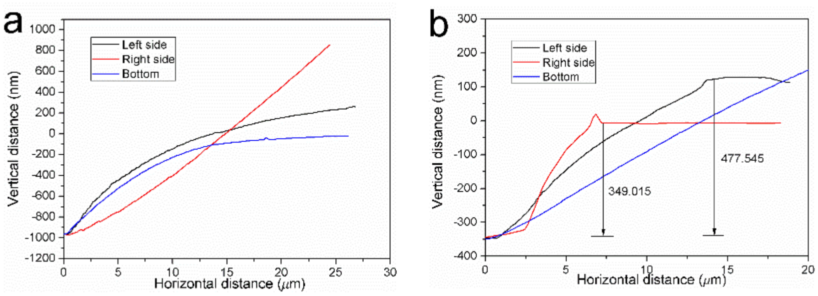

(**a**) (**b**)

Figure 8. Height profile images of etch pit (**a**) and triangular pit (**b**) measured by AFM.

The structure of etch pits is similar to the triangular pits observed in Figures 3 and 5, similar structures were also founded under different levels of supersaturation, as shown in Figure 7c–f, Figure 8b shows the height profile of triangular pit in Figure 7c, the height of the three faces also shows an increasing trend from the bottom to the outside, but smaller than etch pits and elementary steps bunching and bending were observed in these structures. The formation of etch pits is due to the interaction of surface dislocation line outcrops with corrosives, the shape of the pit is related to the crystal plane of the crystal surface, the shape of etch pits on the (101) face of KDP is triangle funnel [33]. According to the similarity of the shape and the convergence and bending of the elementary steps, it can be speculate that the triangular pit is the structure of dislocation line outcrop, the existence of dislocation line makes elementary steps bunched and bended to connect each other in this region.

3.4. Crystal Growth

The growth of larger-size KDP crystals in [101] direction was also performed by rapid growth method, as shown in Figure 9a,b,d. The crystal has two pyramidal sectors, the top one is larger than the bottom part, one face in each pyramidal sector is parallel to the growth platform (Figure 9e). Crystals (a, b) have high transparency, no inclusion formation or microdefect was observed during the growth process; the detailed growth parameter is shown in Table 1.

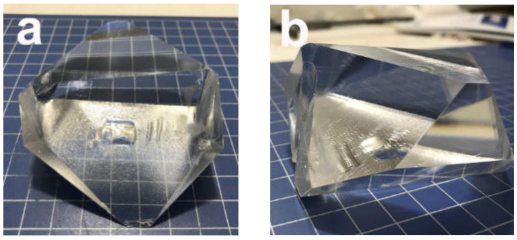

(**a**) (**b**)

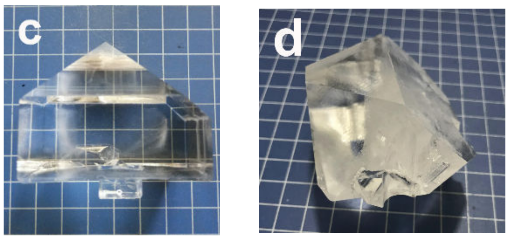

(**c**) (**d**)

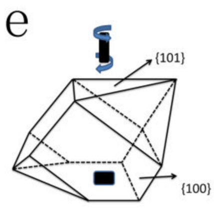

(**e**)

Figure 9. Photos of KDP crystals: (**a**) [101] orientation, 12 mm/day (**b**) [101] orientation 14 mm/day (**c**) Z-cut, 12 mm/day (**d**) [101] orientation 16 mm/day (**e**) schematic diagram of [101] orientation crystal.

Figure 9c is a photo of z-cut KDP crystals grown under the same parameter as crystal in Figure 9a, inclusion and spontaneous nucleation appeared during the growth process, it has been reported that inclusions occur more frequently when the rotation rate is low. During the crystal growth experiments, the probability of inclusion formation increased a lot when the rotation reduced from 77 rpm to 30 rpm. Compared to z-cut crystal growth, [101] direction growth makes the solution distribute more uniformly under the same rotation speed and supersaturation, no inclusion and spontaneous nucleation were observed. When the growth rate increased to 14 mm/day, high transparent KDP crystal was also obtained, as shown in Figure 9b, it grew very fast under this supersaturation, the crystal surface was flat and no convex or concave macrostructure was founded, the prismatic face grew so fast that the platform support was surrounded by the prismatic sector and resulted in the concave structure on the edge. Due to the blocking of solution fluid by the support of platform, the growth rate on both sides of the crystal was different.

Table 1. Growth parameters of KDP crystals.

Serial Number	Rotation Speed/rpm	Growth Rate/mm/day	Temperature Region/°C	Growth Period/day	Crystal Size/mm
a	30	12	55.0–36.3	6	42 × 65 × 72
b	30	14	55.3–35.7	5	38 × 63 × 60
c	30	12	55.5–44.0	5	59 × 54 × 55
d	30	16	54.5–42.1	4	34 × 58 × 55

When the growth rate reached 16mm/day, the supersaturation of the solution was very high, as the crystal size increases, inclusion, crack and spontaneous nucleation occurred on the crystal surface (Figure 9d), which may be evolved from irregular structures at high supersaturation, so during the growth of [101] direction KDP crystal at low rotation rate, it is necessary to keep the supersaturation at a proper range.

3.5. Performance Characteration

3.5.1. Optical Spectrum Transmittance

Optical spectrum transmittance is an important performance index to reflect the interaction between the internal structure of the crystal and light waves, structural defects and impurity ions can lead to an increase of absorption and result in decrease of optical transmittance. To further understand the optical transmittance of KDP crystals grown in [101] direction, crystals were cut into 10mm z-cut wafers, after precision polishing, spectrum transmittance was measured from 200 nm to 1800 nm by UV-infrared spectrophotometer at room temperature, the optical transmission spectra is shown in Figure 10. It can be seen that crystals have high transmittance in the visible-infrared spectra range, the obvious difference occurs in the ultraviolet region, pyramidal sector and prismatic sector show different tendency as the wavelength decreases, pyramidal area slightly drops but still maintains over 54.8% transmittance at 200 nm, the transmittance in the prismatic area gradually decreases and maintains a low transmittance at 200 nm, this may be related to the selective absorption of metal cations by the crystal prismatic structure [31,34], the transmittance of the crystal at 355 nm remains above 82.6%, no obvious absorption peak was found during the measurement process.

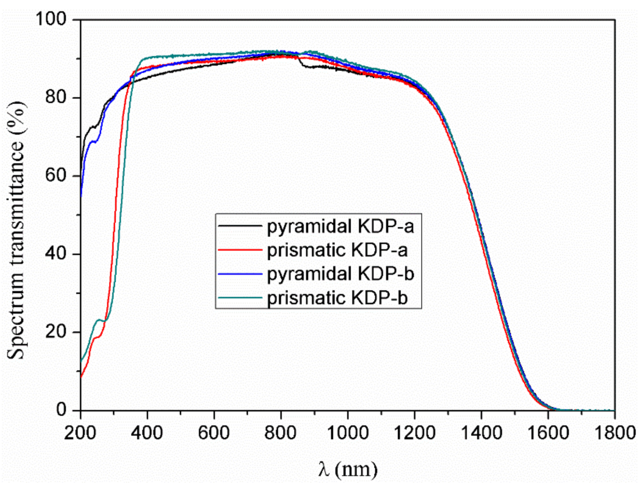

Figure 10. Optical transmittance of KDP crystals grown in [101] direction.

3.5.2. Crystalline Perfection

To further study the crystalline perfection of [101] orientation KDP crystals grown at low rotation rate, a high-resolution X-ray diffractometer was used to record the rocking curves [35] of (001) faces. Crystals were cut into wafers of 2 mm thickness, the face to be tested was precisely polished and then adsorbed on the platform for testing, the recorded rocking curves are shown in Figure 11. The shape of rocking curve is a unique peak with high diffraction intensity and the curve is smooth and symmetrical, which means that the crystalline perfection is very good and no other irregular structure exits. It was found that the presence of internal stress would widen the full width at half maximum(FWHM) [36], the theoretical FWHM value of the (001) plane is 10.8 arc sec, the real FWHM of KDP crystals grown in [101] direction is 16.8116 and 18.4436 arc sec respectively, which means that there is a slight stress inside the crystals during the growth process. The reason for the difference in FWHM of KDP a and b may be due to the degree of supersaturation, high supersaturation leads to faster crystal growth and internal stress increase which make the FWHM widen.

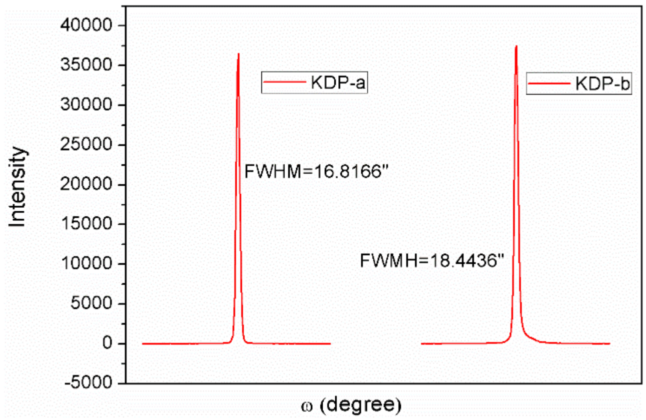

Figure 11. Rocking curves recorded for (001) faces of [101] direction KDP crystals.

3.5.3. Laser Damage Threshold

As an important optical device for electro-optic modulation and frequency conversion in high power laser beam path, high laser damage resistance is a necessary. To measure the laser damage threshold of KDP crystals grown in [101] direction, crystals were cut into plates of 10mm thickness in [001] direction, after precision grinding and polishing process under the same conditions, 1-on-1 mode was used to evaluated the laser damage threshold. Over 10 sites were chosen randomly under one laser energy, He-Ne laser was used as imaging background light for CCD camera to capture the formation of damage, the laser energy was increased gradually and the damage probability was counted until 100%, the laser fluence of 0% damage probability is chosen as the laser damage threshold of the crystal, the test result is shown in Table 2.

Table 2. One-on-one laser damage threshold of different orientation KDP crystals.

Serial Number	Growth Parameter	Laser Parameter	1-on-1 Laser Damage Threshold (J/cm2)
a	[101], 12 mm/day, 30 rpm	1064 nm, 8.4 ns	21.5
b	[101], 14 mm/day, 30 rpm	1064 nm, 8.4 ns	21
d	z-cut, 12 mm/day, 77 rpm	1064 nm, 8.4 ns	21

During the laser damage test, the damage points are located inside the crystal, no surface damage was observed and crystal plates have high homogeneity in damage resistance. Table 2a and b are KDP crystals grown in [101] direction under different supersaturation, Table 2d is KDP crystal without inclusion grown in [001] direction under 77 rpm rotation rate. It can be seen that the difference of laser damage threshold between them is very small, KDP crystals grown in [101] direction under high supersaturation and 30rpm rotation rate can achieve the same laser damage threshold as Z-cut crystal grown under 77 rpm rotation rate.

4. Conclusions

To investigate the causes of inclusion and avoid the formation of it more effectively under low rotation rate, the hydrodynamic condition near the crystal was changed by changing the growth orientation of the crystal, [101] direction KDP crystals were grown by the point seed rapid growth method, growth of inclusion-free crystals was achieved at low rotation speed and the crystals can withstand higher supersaturation without inclusions generation. The optical performance characterization of crystals grown under high supersaturation shows that the crystals have good optical transmittance, crystalline perfection, and laser damage threshold is as good as the z-cut KDP crystals grown at high rotation speed.

AFM shows the micromorphology of (100) and (101) faces of [101] direction KDP crystals under different levels of supersaturation, the height of macrosteps on (100) faces increases with the increase of supersaturation. Uneven distribution of supersaturation and insufficient flow rate caused uneven arrangement of macrosteps heights and widths and increased the instability of interface when the supersaturation was high. The elementary steps on (101) faces have no tendency to converge under low supersaturation, the only steps converge were found in the triangular pit, dislocation outcrops caused the convergence and bending of the nearby elementary steps. Insufficient flow rate and high supersaturation gradient caused elementary steps to aggregate and form irregular microstructures, these unstable structures were composed of elementary steps, two-dimensional step platforms and two-dimensional cores, which have large slopes. The continued evolution of these instable structures will reduce the stability of the interface and cause crystals to form defects. Therefore, during the growth of KDP crystals at low rotation rate, the hydrodynamic condition around the crystal can be changed by using the [101] direction point seeds, solutes can be more uniformly distributed on the surface of the crystal and the interface instability can be reduced. Meanwhile, proper supersaturation must be maintained to avoid losing the stability of the interface.

Author Contributions: M.Q. and X.X. designed the experiment, M.Q. performed the experiment and prepared the samples. G.Y. and W.C. performed the measurements. X.X. and B.W. provided theoretical support, M.Q. wrote the article. All authors have read and agreed to the published version of the manuscript.

Funding: This research was funded by State Key Laboratory of Crystal Materials, grant number ZTD-2018-01.

Conflicts of Interest: The authors declare no conflict of interest.

References

1. Zaitseva, N.; Carman, L. Rapid Growth of KDP-Type Crystals. *Prog. Cryst. Growth Charact. Mater.* **2001**, *43*, 1–118. [CrossRef]
2. Chernov, A.A.; Zaitseva, N.P.; Rashkovich, L.N. Secondary Nucleation Induced by the Cracking of a Growing Crystal: KH_2PO_4 (KDP) and $K(H,D)_2PO_4$ (DKDP). *J. Cryst. Growth* **1990**, *102*, 793–800. [CrossRef]
3. Zaitseva, N.P.; De Yoreo, J.J.; DeHaven, M.R. Rapid growth of large-scale (40–55 cm) KH2PO4 crystals. *J. Cryst. Growth* **1997**, *180*, 255–262. [CrossRef]
4. Brooks, R.; Horton, A.T.; Torgesen, J.L. Occlusion of Mother Liquor in Solution-Grown Crystals. *J. Cryst. Growth* **1968**, *2*, 279–283. [CrossRef]
5. Rashkovich, L.N.; Shekunov, B.Y. Morphology of Growing Vicinal Surface; Prismatic Faces of ADP and KDP Crystals in Solutions. *J. Cryst. Growth* **1990**, *100*, 133–144. [CrossRef]
6. Slaminko, P.; Myerson, A.S. The Effect of Crystal Size on Occlusion Formation during Crystallization from Solution. *Aiche J.* **1981**, *27*, 1029–1031. [CrossRef]
7. Brice, J.C.; Bruton, T.M. The Stability of Facets on Growing Crystals. *J. Cryst. Growth* **1974**, *26*, 59–60. [CrossRef]

8. Rodriquez, R.; Aguiló, M.; Tejada, J. Unstable Growth of ADP Crystals. *J. Cryst. Growth* **1979**, *47*, 518–526. [CrossRef]
9. Chernov, A.A. Formation of Crystals in Solutions. *Contemp. Phys.* **1989**, *30*, 251–276. [CrossRef]
10. Potapenko, S.Y. Morphological Instability of Steps during Crystal Growth from Solution Flow. *J. Cryst. Growth* **1996**, *158*, 346–358. [CrossRef]
11. Potapenko, S.Y. Formation of Solution Inclusions in Crystal under Effect of Solution Flow. *J. Cryst. Growth* **1998**, *186*, 446–455. [CrossRef]
12. Robey, H.F.; Potapenko, S.Y. Ex Situ Microscopic Observation of the Lateral Instability of Macrosteps on the Surfaces of Rapidly Grown KH_2PO_4 Crystals. *J. Cryst. Growth* **2000**, *213*, 355–367. [CrossRef]
13. Robey, H.F.; Maynes, D. Numerical Simulation of the Hydrodynamics and Mass Transfer in the Large Scale, Rapid Growth of KDP Crystals. Part 1: Computation of the Transient, Three-Dimensional Flow Field. *J. Cryst. Growth* **2001**, *222*, 263–278. [CrossRef]
14. Robey, H.F. Numerical Simulation of the Hydrodynamics and Mass Transfer in the Large Scale, Rapid Growth of KDP Crystals—2: Computation of the Mass Transfer. *J. Cryst. Growth* **2003**, *259*, 388–403. [CrossRef]
15. Bordui, P.F.; Motakef, S. Hydrodynamic Control of Solution Inclusion during Crystal Growth of KTiOPO4 (KTP) from High-Temperature Solution. *J. Cryst. Growth* **1989**, *96*, 405–412. [CrossRef]
16. Vartak, B.; Yeckel, A.; Derby, J.J. Time-Dependent, Three-Dimensional Flow and Mass Transport during Solution Growth of Potassium Titanyl Phosphate. *J. Cryst. Growth* **2005**, *281*, 391–406. [CrossRef]
17. Balamurugan, S.; Ramasamy, P. Bulk Growth of <101> KDP Crystal by Sankaranarayanan—Ramasamy Method and Its Characterization. *Mater. Chem. Phys.* **2008**, *112*, 1–4. [CrossRef]
18. Dinakaran, S.; Verma, S.; Das, S.J.; Bhagavannarayana, G.; Kar, S.; Bartwal, K.S. Investigations of Crystalline and Optical Perfection of SHG Oriented KDP Crystals. *Appl. Phys. A* **2010**, *99*, 445–450. [CrossRef]
19. Sharma, S.K.; Verma, S.; Singh, Y.; Bartwal, K.S.; Tiwari, M.K.; Lodha, G.S.; Bhagavannarayana, G. Investigations of Structural Defects, Crystalline Perfection, Metallic Impurity Concentration and Optical Quality of Flat-Top KDP Crystal. *Opt. Mater.* **2015**, *46*, 329–338. [CrossRef]
20. Tu, H.; Zhao, Y.; Yue, Y.; Fan, F.; Hu, Z. Shape-Controlled Growth and Characterization of a Large KDP. *Cryst. Crystengcomm* **2015**, *17*, 6669–6673. [CrossRef]
21. He, Y.; Zeng, J.; Wu, D.; Su, G.; Yan, M. New Technology of KDP Crystal Growth. *J. Cryst. Growth* **1996**, *169*, 196–198. [CrossRef]
22. Salo, V.I.; Voronov, A.P.; Tkachenko, V.F.; Babenko, G.N.; Makoveev, A.V. Growth of KDP Single Crystal Blocks in Defined Crystallographic Direction. *J. Cryst. Growth* **2011**, *337*, 13–19. [CrossRef]
23. Thomas, T.N.; Land, T.A.; Martin, T.; Casey, W.H.; DeYoreo, J.J. AFM Investigation of Step Kinetics and Hillock Morphology of the {100} Face of KDP. *J. Cryst. Growth* **2004**, *260*, 566–579. [CrossRef]
24. Chernov, A.A.; Rashkovich, L.N. Spiral Crystal Growth with Nonlinear Dependence of Step Growth Rate on Supersaturation; the {110} Faces of KH_2PO_4 Crystals in Aqueous Solution. *J. Cryst. Growth* **1987**, *84*, 389–393. [CrossRef]
25. Voronkov, V.V.; Rashkovich, L.N. Step Kinetics in the Presence of Mobile Adsorbed Impurity. *J. Cryst. Growth* **1994**, *144*, 107–115. [CrossRef]
26. Land, T.A.; Martin, T.L.; Potapenko, S.; Palmore, G.T.; De Yoreo, J.J. Recovery of Surfaces from Impurity Poisoning during Crystal Growth. *Nature* **1999**, *399*, 442–445. [CrossRef]
27. Chernov, A. Modern Crystallography III. *Cryst. Growth* **1984**, *36*, 209. [CrossRef]
28. Robey, H.F.; Potapenko, S.Y.; Summerhays, K.D. "Bending" of Steps on Rapidly Grown KH_2PO_4 Crystals Due to an Inhomogeneous Surface Supersaturation Field. *J. Cryst. Growth* **2000**, *213*, 340–354. [CrossRef]
29. De Yoreo, J.J.; Burnham, A.K.; Whitman, P.K. Developing KH_2PO_4 and KD_2PO_4 Crystals for the World's Most Power Laser. *Int. Mater. Rev.* **2002**, *47*, 113–152. [CrossRef]
30. De Yoreo, J.J.; Land, T.A.; Lee, J.D. Limits on Surface Vicinality and Growth Rate Due to Hollow Dislocation Cores on KDP { 101 }. *Phys. Rev. Lett.* **1997**, *78*, 4462–4465. [CrossRef]
31. De Vries, S.A.; Goedtkindt, P.; Bennett, S.L.; Huisman, W.J.; Zwanenburg, M.J.; Smilgies, D.-M.; De Yoreo, J.J.; van Enckevort, W.J.P.; Bennema, P.; Vlieg, E. Surface Atomic Structure of KDP Crystals in Aqueous Solution: An Explanation of the Growth Shape. *Phys. Rev. Lett.* **1998**, *80*, 2229–2232. [CrossRef]
32. Coriell, S.R.; Murray, B.T.; Chernov, A.A.; McFadden, G.B. Step Bunching on a Vicinal Face of a Crystal Growing in a Flowing Solution. *J. Cryst. Growth* **1996**, *169*, 773–785. [CrossRef]

33. Yoreo, J.J.D.; Vekilov, P.G. Principles of Crystal Nucleation and Growth. *Rev. Mineral. Geochem.* **2003**, *54*, 57–93. [CrossRef]
34. Ramasamy, G.; Bhagavannarayana, G.; Meenakshisundaram, S. The Concentration Effects of S-, p-, d- and f-Block Element Doping on the Growth, Crystalline Perfection and Properties of KDP Crystals. *CrystEngComm* **2012**, *14*, 3813–3819. [CrossRef]
35. Lal, K.; Bhagavannarayana, G. A High-Resolution Diffuse X-Ray Scattering Study of Defects in Dislocation-Free Silicon Crystals Grown by the Float-Zone Method and Comparison with Czochralski-Grown Crystals. *J. Appl. Cryst.* **1989**, *22*, 209–215. [CrossRef]
36. Bhagavannarayana, G.; Parthiban, S.; Meenakshisundaram, S. An Interesting Correlation between Crystalline Perfection and Second Harmonic Generation Efficiency on KCl- and Oxalic Acid-Doped ADP Crystals. *Cryst. Growth Des.* **2008**, *8*, 446–451. [CrossRef]